11th World Congress on Computational Mechanics (WCCM XI)
5th European Conference on Computational Mechanics (ECCM V)
6th European Conference on Computational Fluid Dynamics (ECFD VI)
E. Oñate, J. Oliver and A. Huerta (Eds)

ULTRASONIC IMAGE RECONSTRUCTION OF INTERNAL DEFECTS DERIVED BY EMAT USING TRUNCATED SINGULAR VALUE DECOMPOSITION

YOSHIHIRO NISHIMURA*,TAKAYUKI SUZUKI*, KATSUMI FUKUDA†, MASATOSHI FUKUTA† AND EIKI IKEDA†

*Advanced Manufacturing Research Institute
National Institute of Advanced Industrial Science and Technology
1-2-1 Namiki Tsukuba, 305-8564 Japan
e-mail: nishimura.yoshihiro@aist.go.jp, e-mail: suzuki-takayuki@aist.go.jp

†Tokyo National College of Technology
1220-2 Kunugida Hachioji Tokyo, 193-0997 Japan
e-mail: fukuda@tokyo-ct.ac.jp, e-mail: as13605@tokyo-ct.ac.jp, e-mail: as14602@tokyo-ct.ac.jp

Key words: Electromagnetic Acoustic Transducer, Ultrasonic Test, Inverse Problem Solving, Truncated Singular Value Decomposition

Abstract. Electromagnetic Acoustic Transducer is contact-free Ultrasonic Testing and convenient for high-speed scanning of inspected sample. EMAT probes are usually larger than internal defects. Truncated Singular Value Decomposition methods are conducted to derive internal defect images. Relations between truncation index k and reconstructed images were presented.

1 INTRODUCTION

Electromagnetic Acoustic Transducers (EMATs) are used in a contact-free non-destructive testing (NDT) method using ultrasonic waves. They are useful for high-speed scanning of inspected materials or for scanning high temperature materials. The images of internal defects derived by scanning the upper surface of an inspected sample are blurred because EMAT probes are usually larger than ordinary piezoelectric probes and an EMAT probe cannot focus an acoustic wave on a point. Aperture-synthesis [1][2] and Inverse problem-solving approaches can effectively derive clear images of internal defects but their response function matrix often become singular and cannot be solved for Inverse problem solving. To apply these methods, further investigation of the relations between the probe size and defect size is required.

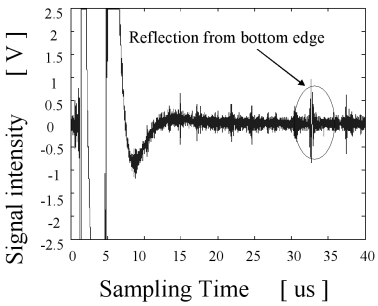

Figure 1: As-received wave form derived b EMAT

2 EMAT Imaging

An EMAT output is acquired as a time series of echo signals, similar to that acquired by a piezoelectric transducer. Figure 1 depicts a signal from a chromium molybdenum steel (SCM415) sample covered with oxide skin observed by EMAT using the magnetostrictive effect. The output presented in Figure 1, which was sampled by an analog-digital converter at 400MHz, is too noisy due to the Barkhausen effect to distinguish reflection waves from noise. The noise can be reduced by statistical averaging (time-based averaging [3], 1D-position-based averaging [4], 3D-position-based averaging [4]).

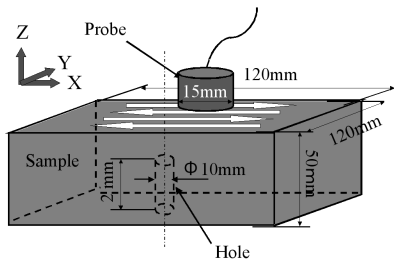

Figure 2: Probe and Sample

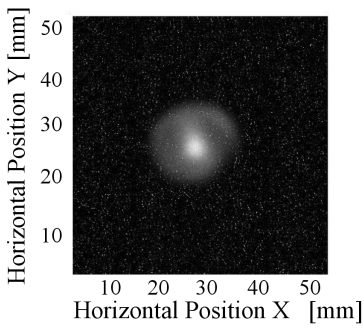

Figure 3: C-scope Image reconstructed from as-received waveforms

3 SIGNAL PROPAGATION THEORY OF EMAT

Let us consider the system depicted in Figure 4. The distribution of internal defects corresponds to that $\rho(\vec{X}+\vec{x})$ of the reflection coefficient in the inspected sample. The relation between the output signal $w(\vec{X},t)$ of the EMAT probe and the distribution of the reflection coefficient $\rho(\vec{X}+\vec{x})$ from internal defects can be calculated using Equations (1) and (2). (Figure 4) Here, $h(\vec{x_1},t)$ is the response function of the probe. $\vec{X}$ is the global coordinate $(X,Y,0)$ of the center of the probe. $\vec{x_0}$ and $\vec{x_2}$ are the local coordinates

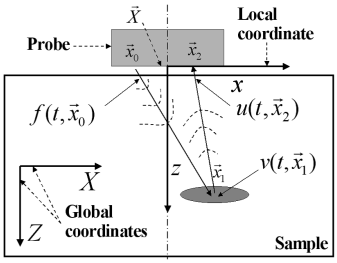

Figure 4: Wave propagation from EMAT probe

(x_0, y_0) , $(x_2, y_2, 0)$ of the bottom surface of the probe. The local coordinate (0, 0, 0) is the center of the bottom surface of the EMAT probe. $\vec{x_1}$ is a local coordinate (x_1, y_1, z_1) within the inspected sample. $f(t)$ is a time series of the signal emitted from the probe. c is the velocity of an acoustic wave. is the damping coefficient.

$$w(\vec{x}, t) = \int \rho(\vec{X} + \vec{x}) \cdot h(\vec{x_1}, t) dx_1 dy_1 dz_1 \tag{1}$$

$$h(\vec{x_1}, t) = \int \frac{f(t - \frac{|\vec{x_2} - \vec{x_1}| + |\vec{x_0} - \vec{x_1}|}{c})}{|\vec{x_2} - \vec{x_1}| \cdot |\vec{x_0} - \vec{x_1}|} \cdot e^{-\alpha(|\vec{x_2} - \vec{x_1}| + |\vec{x_0} - \vec{x_1}|)} dx_0 dy_0 dx_2 dy_2 \tag{2}$$

Equation (1) can be Fourier transformed to Equation (3).

$$W(t, \vec{S}) = \int H(t, \vec{S}, z_1) \cdot P(\vec{S}, z_1) dz_1 \tag{3}$$

Here, $\vec{S} = (S, T, 0)$ and $W(t, \vec{S})$, $P(\vec{s}, z_1)$ and $H(t, \vec{S}, z_1)$ are defined as Equations (4-6). Damping coefficient α can be assumed to be mostly 0 for defects sufficiently near the probe

$$W(t, S, T) = \int w(t, x_2, t_2) \cdot e^{-(Sx_2 + Ty_2)} dx_2 dy_2 \tag{4}$$

$$H(t, S, T, z_1) = \int h(t, x_1, y_1, z_1) \cdot e^{-(Sx_1 + Ty_1)} dx_1 dy_1 \tag{5}$$

$$P(S, T, z_1) = \int \rho(x_1, y_1, z_1) \cdot e^{-(Sx_1 + Ty_1)} dx_1 dy_1 \tag{6}$$

Equation (3) can be presented as Equation (7) in matrix form. Here, the horizontal resolution is $N = N_x \times N_y$. Calculating probe output $W(t, S)$ from reflection coefficients $P(\vec{S}, z_1)$ is not difficult because the response function matrix $H(t, \vec{S}, z_1)$ is diagonal. However, it is not always easy to calculate reflection coefficients $P(\vec{S}, z_1)$ from the probe

output $W(t, \vec{S})$ because of the singularity of the response matrix. Here, $W_{t\vec{S}} = W(t, \vec{S})$, $P_{\vec{S}z_1} = P(\vec{S}, z_1)$, $H_{t\vec{S}z_1} = H(t, \vec{S}, z_1)$

$$\begin{pmatrix} W_{t\vec{0}} \\ \vdots \\ W_{tt\vec{S}} \\ \vdots \\ W_{tt\vec{S_N}} \end{pmatrix} = \int \begin{pmatrix} H_{t\vec{0}z_1} & 0 & \cdots & \cdots & 0 \\ 0 & \ddots & 0 & \cdots & \vdots \\ \vdots & 0 & H_{t\vec{s}z_1} & 0 & \vdots \\ \vdots & \cdots & 0 & \ddots & 0 \\ 0 & \cdots & \cdots & 0 & H_{t\vec{S_N}z_1} \end{pmatrix} \begin{pmatrix} P_{\vec{0}z_1} \\ \vdots \\ P_{\vec{S}z_1} \\ \vdots \\ P_{\vec{S_N}z_1} \end{pmatrix} dz_1 \tag{7}$$

When horizontal resolution N is large, the condition number of the response function matrix H become large. The high degree of diagonal elements is likely to cause large computational errors in inverse solving of Equation (3) due to magnification of the error of double-precision floating-point calculations .

4 IMAGE RECONSTRUCTION FROM EMAT SIGNAL

The response function $h(\vec{x_1}, t)$ can be calculated from $f(t)$ using Equation (2). Figure 5 presents the signal waveform $f(t)$ measured from the sample depicted in Figure 2.

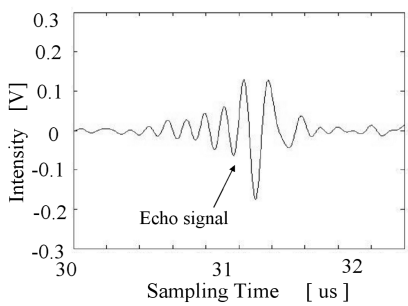

Figure 5: Echo signal $f(t)$ used to calculate the response

Equation (3) can be solved using Truncated Singular Value Decomposition (TSVD).[5][6] Figures 6 (a-h) depict the relation between reconstructed images of hole defects of 10mm diameter and the truncation index k of truncated singular decomposition matrix H_d. Here, Figure 6 (a) is an as-received C-scope image and cross-section of a defect calculated from a 10mm-diameter numerical defect model. Figures 6 (b-h) are reconstructed using truncated singular value decomposition matrix H_d whose truncation index is k.

When the truncation index k is small, images of defect are blurred. As the truncation index k become large , images of defect become clear but high frequency noises become strong. Then, the best condition number for image reconstruction is thought to be located between 100 and 150. Figures 7 (a-d)) presents images of the reflection intensity distribution calculated for the numerical hole defect model. Their diameters are 10mm, 6mm,

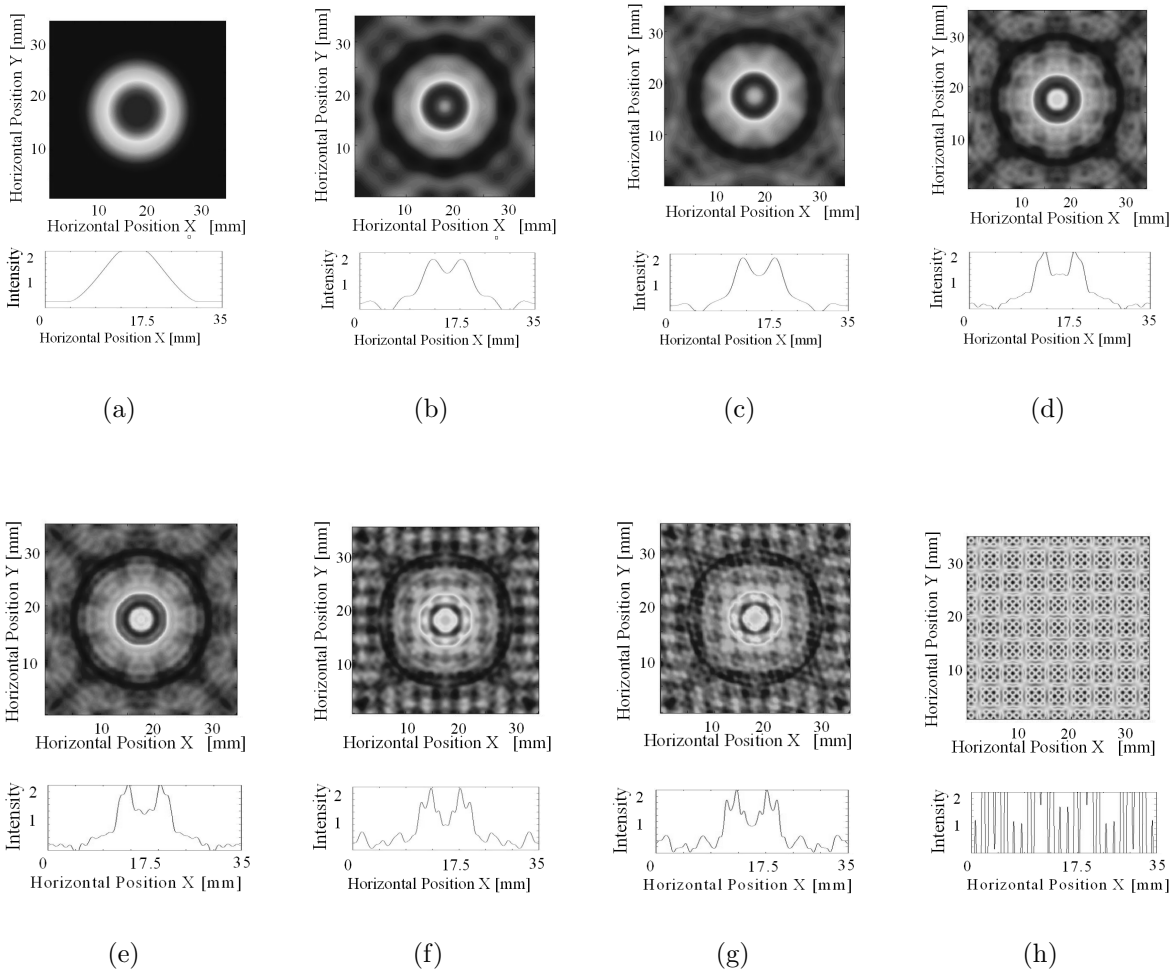

Figure 6: Dependence of defect images on truncation index k. (a) As-received (b) k=20 (c) k=50 (d) k=100 (e) k=150 (f) k=200 (g) k=220 (h) k=250

3mm and 1.5mm. The intensity of the defect images decreases as the defect becomes small, but their sizes doesn ' t change.

Figures 8 (a-d) present images reconstructed for hole defects presented in Figure 7 using TSVD with the truncation index k=120. All sizes of hole defects could be reconstructed quite clearly except high-frequency noise. The sizes of hole defects were reproduced exactly . The sample hole defects of four different diameter depicted in Figure 9 was prepared and measured by EMAT probe. Figure 10 (a) presents an as-received image reconstructed from the probe output with noise reduced by the statistical method [1] for 10mm hole defect in the sample in Figure 9. Much noise can be seen around the hole defect. Figure 11 (b) presents an image of a 10mm hole defect reconstructed using TSVD.

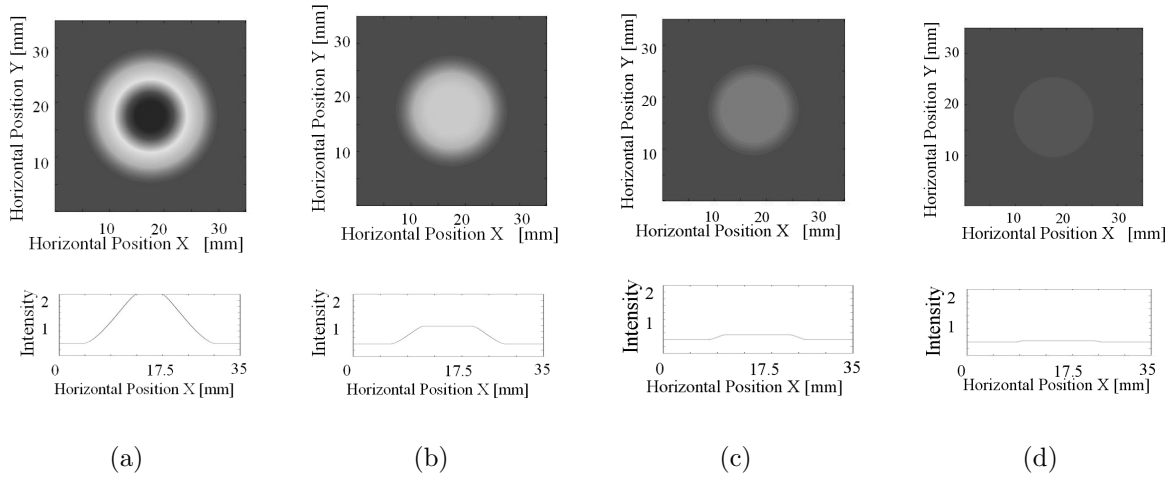

Figure 7: As-received images of different diameter of hole defects derived by numerical calculation (a) d=10mm (b) d=6mm (c) d=3mm (d) d=1.5mm

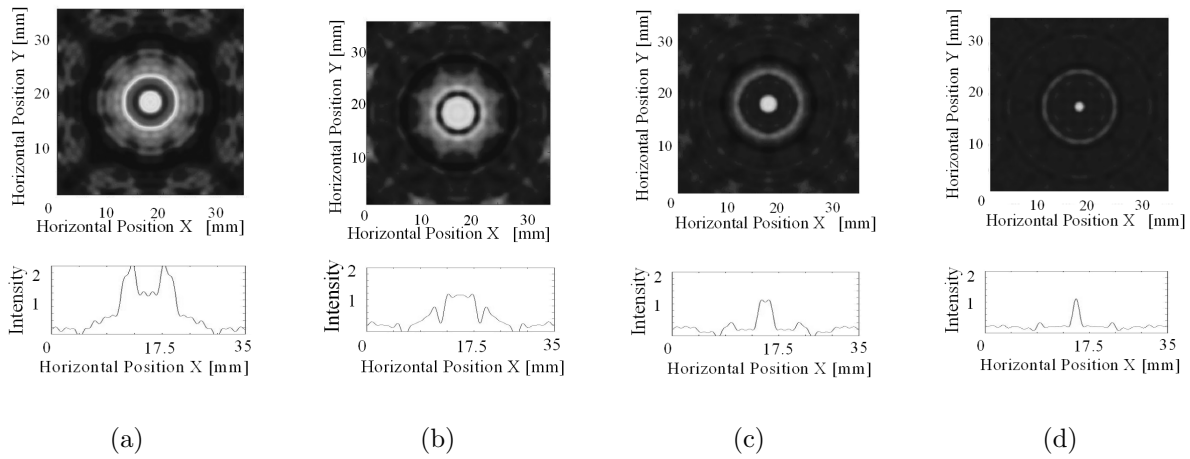

Figure 8: Calculated images of hole defects using TSVD with truncation index k=120 (a) d=10mm (b) d=6mm (c) d=3mm (d) d=1.5mm

The diameter of the hole defect was reproduced quite exactly, but noise surrounding the defect was reproduced as strong high-frequency noise.

Figures 11 (a) and (b) present images of the 6mm hole defect. High-frequency noise became strong because the intensity of the reflection is lower than that of the 10mm hole defect.

A C-scope image of a hole defect 1.5mm in diameter could not be seen because of the

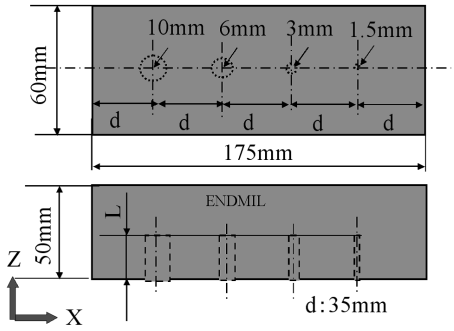

Figure 9: Inspected sample with different hole defects

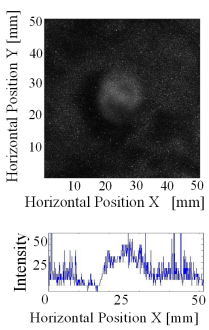

(a)

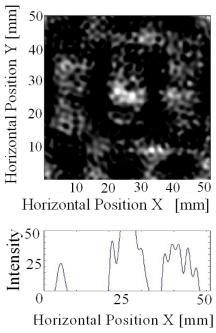

(b)

Figure 10: C-Scope images of 10mm hole defects. (a) As-received. (b)Reconstructed

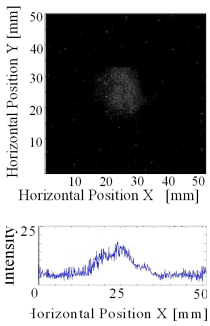

(a)

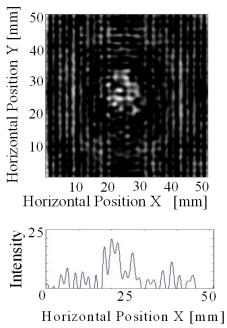

(b)

Figure 11: C-Scope images of 6 mm hole defects. (a) As-received (b) Reconstructed

very small echo signal.

5 CONCLUSION

- The statistical method used could successfully remove noises from signal generated by internal defects.
- The response function could be calculated based on a waveform. The reflection intensity distribution image of the internal defects model of various diameters was calculated, and the relation between measured images and original defect images was investigated.
- Solving original defect image from probe output data using TSVD was investigated. The relation between the condition number and the image reconstructed using TSVD was shown. Influence of high frequency noise was investigated as well..

- A sample with internal hole defects of different diameters was prepared and measured by EMAT. Images of hole defects derived by EMAT had size and intensity tendencies similar to those derived by numerical calculation.

- The inverse solving method using TSVD was applied to the data measured by EMAT. It was shown that a more exact defect shape can be derived and that large condition number causes high-frequency noise.

Acknowledgements

This research was partially supported by JST Adaptable and Seamless Technology transfer Program A-STEP (AS251Z00124K).

REFERENCES

[1] K. Nakahata, M. Hirohata, and S. Hirose, “Flaw Reconstruction from Scattering Amplitude using Full-waveform Sampling and Processing(FSAP),” Journal of JSNDI, vol. 59, .6, pp. 277-283, 2010.

[2] E. Sato, M. Shiwa, K. Yamashita, A. Sato, M. Koshirae, and K.Kitami, ”Method of Automatic Ultrasonic Inspection by Phased Array System for Graphite Ingot,” JAXA Research and Development Memorandum, JAXA-RM-05-006, 2006.

[3] Nishimura Y.,Sasamoto A., and Suzuki T., Study of Signal processing for EMAT, Material Science Forum, 670, pp.151-157, (2011).

[4] Nishimura Y., Sasamoto A., and Suzuki T., Signal processing of EMAT Using Magnetstrictives by Statistical Method, J.JSAEM,19, pp.531-535., (2011).

[5] A.N.Tikohonov, V.Y.Aresenin, Solution of ill-posed Problems Winston & Sons, Washington, D.C., (1977).

[6] P. Bojarczak, Z. Lukasik, ”Image Deblurring-Winer Filter versus TSVD Approach,” Advances in Electrical and Electronic Engineering, No, 2, Vol. 6, pp. 86-89, 2007.